Biochimica et Biophysica Acta 1837 (2014) 375–384

Contents lists available at ScienceDirect

Biochimica et Biophysica Acta

journal homepage: www.elsevier.com/locate/bbabio

Steady-state kinetics with nitric oxide reductase (NOR): New considerations on substrate inhibition profile and catalytic mechanism

Américo G. Duarte *[,1], Cristina M. Cordas [1], José J.G. Moura, Isabel Moura

Requimte, Centro de Química Fina e Biotecnologia, Departamento de Química, Faculdade de Ciências e Tecnologia, Universidade Nova de Lisboa, Quinta da Torre, 2829-516 Monte de Caparica, Portugal

ARTICLE INFO

Article history:
Received 16 June 2013
Received in revised form 28 December 2013
Accepted 2 January 2014
Available online 9 January 2014

Keywords:
NOR
NO reduction
Enzyme kinetics
Electrochemistry

ABSTRACT

Nitric oxide reductase (NOR) from denitrifying bacteria is an integral membrane protein that catalyses the two electron reduction of NO to N_2O, as part of the denitrification process, being responsible for an exclusive reaction, the N–N bond formation, the key step of this metabolic pathway. Additionally, this class of enzymes also presents residual oxidoreductase activity, reducing O_2 to H_2O in a four electron/proton reaction. In this work we report, for the first time, steady-state kinetics with the *Pseudomonas nautica* NOR, either in the presence of its physiological electron donor (cyt. c_{552}) or immobilised on a graphite electrode surface, in the presence of its known substrates, namely NO or O_2. The obtained results show that the enzyme has high affinity for its natural substrate, NO, and different kinetic profiles according to the electron donor used. The kinetic data, as shown by the pH dependence, is modelled by ionisable amino acid residues nearby the di-nuclear catalytic site. The catalytic mechanism is revised and a mononitrosyl-non-heme Fe complex (Fe^{II}_B-NO) species is favoured as the first catalytic intermediate involved on the NO reduction.

1. Introduction

Bacterial nitric oxide reductase (NOR) is an integral membrane enzyme that catalyses the nitric oxide (NO) reduction to nitrous oxide (N_2O) in a two electron/proton reaction. NORs have been isolated from different denitrifying organisms, such as *Paracoccus denitrificans* [1,2], and several *Pseudomonas* species, such as *stutzeri* [3,4], *aeruginosa* [5] and *nautica* [6], currently known as *Marinobacter hydrocarbonoclasticus* [7]. This enzyme belongs to the bacterial denitrification pathway ($NO_3^- \rightarrow NO_2^- \rightarrow NO \rightarrow N_2O \rightarrow N_2$), where NO_3^- is the electron acceptor, being reduced to N_2 in consecutive redox reactions, mediated by different metalloenzymes [8,9]. The step catalysed by NOR is the most exquisite in the denitrification pathway, since it is when the N–N double bond is formed, being its molecular mechanism the less understood, causing controversy during the last decade [9,10].

NORs belong to the heme-copper oxidases (HCuO) superfamily and can be classified as cNOR, qNOR, and qCuNOR. All NORs contain a 12 transmembrane alpha helixes domain with high structural homology with the HCuO catalytic subunit, with a catalytic di-iron centre instead of a mixed Fe/Cu catalytic centre [8], although different NOR subclasses present distinct electron transfer centres, physiologic electron donors and number of subunits. cNOR are heterodimeric and receive electrons from soluble periplasmic *c*-type cytochromes (or azurin), while qNOR and qCuNOR (presenting a binuclear Cu centre) can be homodimeric and heterodimeric and transfer electrons from the membrane quinol pool for substrate reduction [8,9].

Ps. nautica NOR is purified as a cytochrome *bc* complex, composed by two subunits. The small subunit, the NorC, is anchored to the membrane and carries a low-spin heme *c* with a His-Met coordination. The large subunit, also named the catalytic subunit, harbours a low-spin heme *b*, with a bis-His coordination and an unusual catalytic binuclear iron centre, composed by a heme *b* (heme b_3) magnetically coupled to a non-heme iron (Fe_B) [11–13]. Heme b_3 was considered to be high-spin [12,14]. However, the first resolved crystal structure of the *Ps. aeruginosa* NOR revealed the presence of the proximal His residue coordinating the iron within the catalytic heme along with a μ-oxo bridge between the two catalytic iron atoms [15]. Additionally, Mössbauer spectroscopy performed with the *Ps. nautica* NOR, proved unequivocally that the heme b_3 is low-spin, for both ferric and ferrous states [6].

NORs, as mentioned, are classified as members of the HCuO superfamily. Its catalytic subunits share a strong structural homology, possessing 12 central transmembrane helices and six conserved histidines responsible for anchoring the low-spin electron transfer heme and binuclear catalytic centres. Although, HCuO carry a mixed binuclear Fe/Cu catalytic centre responsible for O_2 reduction, in particular cases, its

Abbreviations: NOR, Nitric oxide reductase; NO, Nitric oxide; N_2O, Nitrous oxide; *Ps*, *Pseudomonas*; KPB, Potassium phosphate buffer; RDE, Rotating disk electrode; SCE, Saturated calomel electrode

* Corresponding author at: Instituto de Tecnologia Química e Biológica/Universidade Nova de Lisboa, Av. da República, Estação Agronómica Nacional, 2780-157 Oeiras, Portugal. Tel.: +351 212948381; fax: +351 212948550.

E-mail addresses: americogduarte@fct.unl.pt (A.G. Duarte), c.cordas@fct.unl.pt (C.M. Cordas), jjgm@fct.unl.pt (J.J.G. Moura), isabelmoura@fct.unl.pt (I. Moura).

[1] Both author contributed equally for this scientific work.

0005-2728/$ – see front matter © 2014 Elsevier B.V. All rights reserved.
http://dx.doi.org/10.1016/j.bbabio.2014.01.001

ability for NO reduction has been observed as well [16,17]. Similarly, besides the NO reduction, NORs have the ability of reducing O_2 to H_2O in a four electron/proton reaction [18–21]. Nevertheless, independently from the substrate, NORs are non-electrogenic, which means that these enzymes are incapable of pumping protons across the plasmatic membrane [22].

The mechanism for NO reduction remains unclear and is still the subject of intense discussion [8,10,23–26]. Currently, the *cis* and *trans*-mechanisms are the two proposed models. The *cis*-mechanism describes the NO reduction by the binding of two NO molecules to the same iron site, while the other iron centre plays a role of electron transfer and/or assist on the catalytic process [6,27,28]. The *trans*-mechanism proposes the binding of one substrate molecule to each of the iron sites of the binuclear centre, with the formation of a $[FeNO]^7{}_2$ complex [5,29–31].

Several attempts have been made to mimic the unique NOR heme/non-heme iron binuclear centre. Besides inorganic model compounds [32] (and references therein), an engineered sperm whale myoglobin was constructed [33,34]. It successfully reproduced the NOR active centre with the magnetic coupling between the two iron sites, but experiments carried out in the presence of NO have shown low reductase activity [33–35]. Recently, Resonance Raman Spectroscopy was used to investigate the NO reduction mechanism in these modified myoglobins, and the formation of a stable heme–NO complex as a reaction intermediate was pointed. However, the authors' own characterisation of the catalytic active form revealed a five-coordinated high-spin heme, considerably different from the six-coordinated low-spin heme b_3 in the native NOR [6,15].

The O_2 reduction mechanism for NORs has not yet been elucidated as well, although it is assumed that only the catalytic heme b_3 is involved, with the possible formation of a ferryl intermediate, similar to what is described for the cytochromes *c* oxidases [36]. Direct electrochemical studies with *Ps. nautica* NOR have shown no changes in the catalytic heme b_3 redox potential under NO turnover [37]. Also, an intense catalytic current near its redox potential, under O_2 turnover was observed. This is consistent with a possible heme b_3-O_2 complex formation, not yet characterised in this class of enzymes. From the voltammetric assays conducted previously with the immobilised *Ps. nautica* NOR, it was possible to attain the redox potential for each of the enzyme metal centre, as well as evaluate the substrate reduction (NO and O_2) [20,37]. From these latest results, a low redox potential for the catalytic Fe_B was observed, suggesting a *cis*-Fe_B mechanism for the NO reduction process [37].

Steady-state kinetics under NO reduction has been reported previously [11,38]. In all the reported studies the high concentration of substrate (in the low micromolar scale) inhibits the enzyme activity. This inhibition was primarily explained by the binding of one substrate molecule to the enzyme's oxidised form, considered as the enzyme's inactive form. This hypothesis was strongly supported by the stability of heme Fe^{III}-nitrosyl compounds [11]. Lachmann and co-workers used flow-flash measurements in single turnover conditions demonstrating that substrate concentration controlled the intramolecular electron transfer (ET) in the NO reduction mechanism and the substrate binding to the inhibition site occurs before the electron redistribution to the catalytic centre [39]. Recently, a theoretical study developed with DFT calculations has indicated a weak interaction between NO and the oxidised binuclear iron centre, suggesting an inhibitory profile caused by nitrate formation from a side reaction [28]. In contrast, other authors have assumed that the inhibition profile was due to the binding of three substrate molecules to the binuclear iron centre of NOR [38]. Such a kinetic mechanism should be revised considering the new insights on the catalytic binuclear iron centre structure and the heme b_3 spin state [6,15].

In this work we report steady-state kinetics, using the *Ps. nautica* NOR, together with its physiological electron donor (cyt. c_{552}), or adsorbing the enzyme to a graphite electrode, that mimics its physiological electron partner, in the presence of NO or O_2 as substrates. The determined kinetic parameters confirm the high affinity and turnover of this enzyme for NO. The use of different electron donor systems allowed us to review the proposed mechanisms and substrate inhibited forms present on the NO reduction process. Also, pH dependence experiments in turnover conditions gave new insights of the influence of ionisable groups close to the catalytic cavity, which may be responsible for the modulation of the chemical environment near the enzyme active site.

2. Materials and methods

2.1. Protein purification

Ps. nautica cells were grown as described by Prudêncio et al. [40]. The NOR enzyme was purified from bacterial membrane extracts and biochemically and spectroscopically characterised, as previously described [6].

Soluble cytochromes (cyt. c_4, c_{549}, c_{551} and c_{552}) were purified from the *Ps. nautica* soluble crude extract, as reported elsewhere [41–46]. Horse heart cytochrome *c* was purchased from *Sigma*. In order to use the cytochromes as the electron donors, pure protein samples were reduced with excess of sodium ascorbate, briefly centrifuged and applied into a His-Trap column (*General Electrics*), equilibrated with 100 mM potassium phosphate buffer (KPB) pH 7.0. The eluted fraction was collected immediately, closed in an anaerobic flask and the atmosphere within was replaced with argon, in order to prevent the heme re-oxidation. The protein concentrations were determined using the correspondent molar extinction coefficients reported in the literature: $\varepsilon_{411\ nm} = 295\ mM^{-1}\ cm^{-1}$ (as isolated NOR) [6] and $\varepsilon_{417\ nm} = 158.94\ mM^{1}\ cm^{-1}$ (reduced cyt. c_{552}) [46].

2.2. Electron transfer under O_2 turnover

Reduced soluble *c*-type cytochromes were mixed with *Ps. nautica* NOR in order to evaluate their efficiency on the direct ET process. The experiments were conducted aerobically in 100 mM KPB pH = 7.0, 0.01% (w/v) n-dodecyl-β-D-maltoside (DDM) with a cytochrome/NOR molar ratio of 100. Spectroscopic changes were monitored at the specific wavelengths for the Soret, alpha and beta peaks of each of the employed cytochromes.

2.3. Protein immobilisation to the graphite electrode surface

The *Ps. nautica* NOR was immobilised on a graphite electrode surface using the solvent casting technique. Volumes from 7 to 14 μL of a 45 μM pure protein sample were applied on the electrode surface. Primarily, the graphite electrode was treated by immersion in a diluted HNO_3 solution, rinsed in deionised water, hand polished with 5, 1 and 0.3 μm alumina, briefly sonicated and finally rinsed with deionised water.

2.4. Direct electrochemical studies

NO and O_2 reduction and the corresponding obtained catalytic currents were investigated using NOR immobilised on a rotating graphite disk electrode (RDE) by linear sweep voltammetry technique. The graphite modified RDE was set as the working electrode, and a platinum wire and a saturated calomel electrode (SCE), were the secondary and reference electrodes, respectively. The three electrode system was connected to a μAUTOLAB potentiostat and the data was acquired with the GPES software. The assays were conducted in a one compartment cell, using as electrolyte solution, a buffer composed by a 20 mM mixture of sodium citrate, 2-(N-Morpholino)ethanesulfonic acid (MES), 4-(2-Hydroxyethyl)piperazine-1-ethanesulfonic acid (HEPES) and N-(1,1dimethyl-2-hydroxyethyl)-3-amino-2-hydroxypropanesulfonic acid (AMPSO), equilibrated at pH 7.6. Catalytic assays performed under

substrate dependence were accomplished using a scan rate of 50 mVs^{-1} and a constant angular speed of 2000 RPM.

The coverage on the electrode surface was determined with cyclic voltammetry (CV) at scan rates from 1 to 5 Vs^{-1}, aiming the surface coverage determination. The voltammograms exhibited the previous characterised heme b_3 redox process, which was used to determine the electrode surface coverage (Γ) [20,37]. All the assays were conducted under atmosphere controlled conditions, inside an anaerobic chamber (MBraum). All the potential values and voltammograms are presented in reference to the normal hydrogen electrode (NHE).

2.5. Steady-state kinetics with the reduced cyt. c_{552}

NO consumption using the reduced cyt. c_{552} in solution was measured with an ISO-NO Mark II electrode, with a 2 mm sensor in an appropriate reaction vessel, as described by Timóteo et al. [6]. The supporting buffer was a 20 mM mixture buffer (see text above) pH 7.6, 0.02% (w/v) DDM, containing 20 μM of reduced *Ps. nautica* cyt. c_{552}. NO aqueous solution was added from a 100 μM (at 20 °C) stock solution as described elsewhere [6,11], and the reaction was started with the addition of the enzyme (70 nM).

O_2 consumption was measured with a modified Clark type electrode (*Hanstech*) in chronoamperometric assays. The platinum electrode was set as the working electrode, the silver as the secondary electrode and a third reference electrode (SCE) was added. The three electrodes were connected to a μAUTOLAB potentiostat and the potential was set constant at −0.7 V vs SCE during all the experiments. Data acquisition and treatment were done with the GPES software. The experiments were conducted anaerobically in a 20 mM mixture buffer (see text above) pH 7.6 0.02% (w/v) DDM with 30 μM of reduced cyt. c_{552}. O_2 was added from a water solution containing the dissolved gas (278 μM at 20 °C) [47], and the reaction was started with the addition of the enzyme (500 nM).

2.6. pH dependence experiments

The pH dependence experiments were done using the immobilised enzyme on the RDE as previously described (see text above). The previous electrolyte solution (20 mM mixture buffer) was equilibrated at different pH values, from 2.5 to 9.7. Different volumes of NO dissolved in water were added to the electrolyte solution, in order to attain a catalytic response for substrate concentration dependence for each pH solution. The data were acquired as reported previously for the steady-state kinetic assays with the immobilised enzyme.

3. Results and discussion

3.1. Direct electron transfer

When immobilised on a graphite electrode, *Ps. nautica* NOR response shows high heterogeneous electron transfer rate constants (k_s) for the four metal centres, where the higher values belong to the binuclear iron centre (129 and 73 s^{-1} for heme b_3 and Fe_B, respectively), indicating an efficient electron transfer between the electrode and the catalytic iron centre [37]. When working with immobilised enzymes it is essential to ensure that these remain in its active state when adsorbed. In this work, NOR remains active when immobilised, since the measured catalytic current increases with the increase of substrate concentration (NO or O_2) and the kinetic parameters determined with the enzyme in solution and immobilised are in the same order of magnitude and comparable with other isolated NORs [6,11] (see Table 1).

3.2. Specificity of the electron donors

Physiologically, cNORs receive electrons from small soluble periplasmic proteins, such as *c*-type cytochromes [15,48], or azurin [24].

Table 1
Kinetic parameters for the NO and O_2 reduction, with different electron donors.

Electron donor	Cyt. c_{552}		Graphite RDE	
Substrate	NO	O_2	NO	O_2
k_{cat} (s^{-1})	30.4 ± 1.7	0.9 ± 0.1	11.56 ± 0.8	n.d.
K_1 (μM)	3.6 ± 0.8	49.1 ± 3.2	1.0 ± n.d. × 10^{-2}	33.4 ± 2.7
K_2 (μM)	6.2 ± 0.7	–	2.2 ± 0.2	–
K_i (μM)	9.7 ± 0.4	56.3 ± 2.8	–	54.3 ± 4.7

n.d. — not determined

Ps. nautica NOR was shown to use electrons delivered from the periplasmic cyt. c_{552} under NO turnover [6,48] and, as expected, the same electron donor is effective under O_2 turnover as it is shown in Fig. 1. From the purified *c*-type cytochromes, the reduced cyt. c_{552} presents the higher re-oxidation rate when in the presence of NOR, in air saturated conditions, confirming its role as the *Ps. nautica* NOR physiological electron donor.

3.3. NO and O_2 reduction at NOR modified electrodes

NO and O_2 consumptions were investigated independently. The kinetic response towards the different substrates (NO and O_2) was evaluated with the bacterial NOR immobilised on the graphite RDE (Fig. 2).

Earlier, Cordas et al. demonstrated a kinetic response for this same enzyme and for the same substrates, but using a modified stationary pyrolytic graphite electrode [20,37]. Now, a rotating disk electrode was used to ensure a convective flow of the dissolved substrate towards the electrode surface, eliminating substrate diffusion issues, and simultaneously allowing the fast product removal away from the immobilised enzyme [49].

Under this experimental setup it is possible to perform steady-state kinetic experiments and evaluate the kinetic profile for each substrate reduction with two distinct electron donor systems: the physiological electron donor — reduced cyt. c_{552} or with an electrochemical one, with the enzyme immobilised to a graphite RDE, mimicking the role of the physiological partner.

In the presence of O_2, a catalytic wave develops starting around 0 V reaching a limiting value around −0.35 V (Fig. 2B). When in the

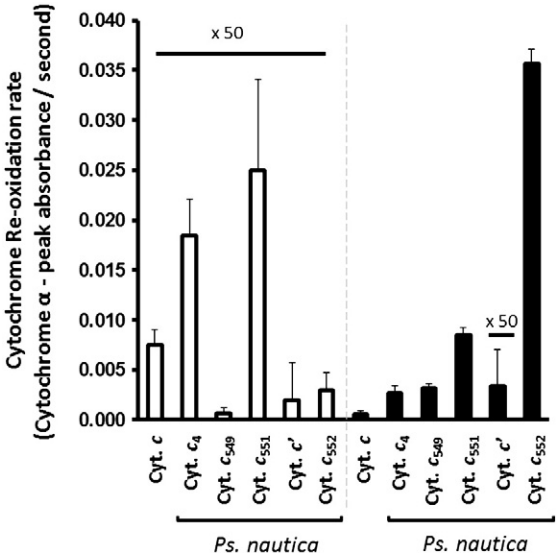

Fig. 1. Horse heart *c*-type cytochrome (Cyt. *c*) and several *Ps. nautica* cytochromes re-oxidation rate without (white bars) or with (black bars) *Ps. nautica* NOR in air saturated conditions (experimental details described in the Materials and methods section). The original version of the figure can be seen in supporting information — Fig. S.1.

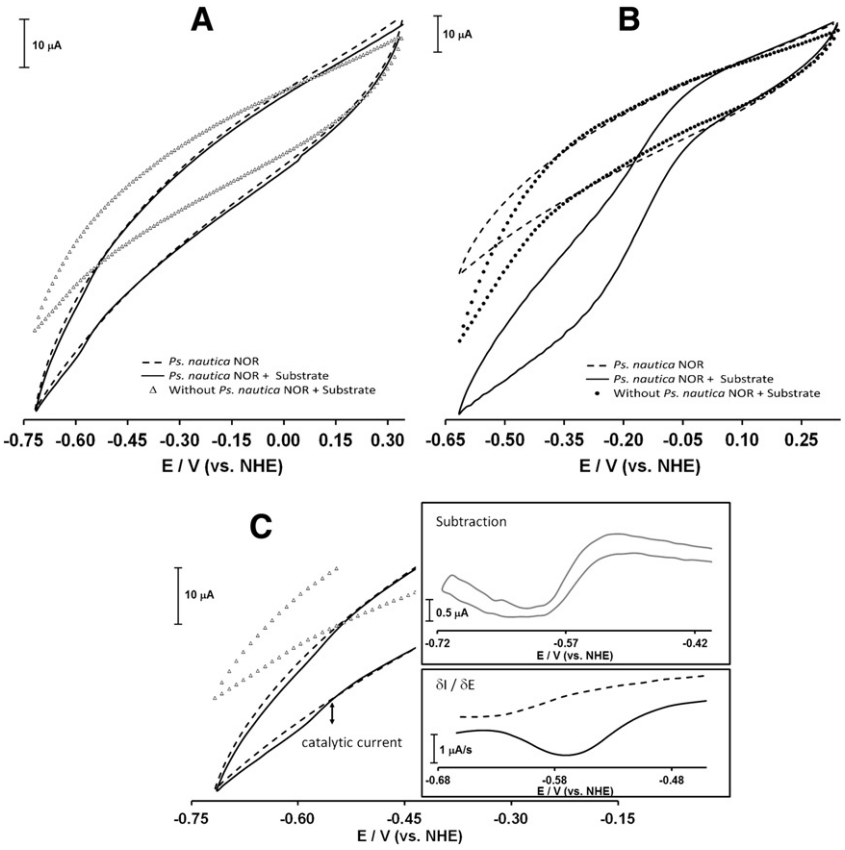

Fig. 2. (A) NO and (B) O_2 reduction using the *Ps. nautica* NOR modified RDE. The cyclic voltammograms were obtained with a $\nu = 50$ mVs^{-1}, $\omega = 5000$ rpm and substrate concentration of 20 and 56 μM for NO and O_2, respectively (electrolyte solution and electrochemical cell composition are described in the Materials and methods section). C — Detail from panel A, indicating catalytic current development under NO turnover, a voltammogram subtraction (*Ps. nautica* NOR-RDE + NO menus *Ps. nautica* NOR-RDE) and the cathodic wave derivative for the experiment with *Ps. nautica* NOR immobilised on RDE in the presence of substrate (black line) and without enzyme in the presence of substrate (dashed line).

presence of NO, also a catalytic current develops, at lower potentials, starting close to −0.45 V and reaching the limiting current near −0.6 V (Fig. 2A). In order to ensure that the observed enhanced current is not due to the substrate reduction at the electrode surface, the subtraction of the control voltammograms and the derivatives of the cathodic waves (obtained in the presence of NO and O_2) and controls were performed (Figs. 2 and S.2 in supporting information). In the absence of substrates or adsorbed enzyme, no catalytic currents are observed. In both cases, either with O_2 or NO as substrate, sigmoidal shape and plateau limiting currents are attained, which are characteristic of steady-state electrochemical conditions. Clearly, the waves developed in the presence of NO and O_2 are distinct, not only in terms of the potential values where they start to develop but also in their shape and intensity (Fig. 2). This is in agreement with the results reported earlier, with the same enzyme adsorbed to a stationary pyrolytic graphite electrode [37]. The variation on the potential value corresponding to the catalytic current initial development can be explained by the two catalysis' different mechanisms, namely with which of the Fe sites is involved in the substrate reduction. NO reduction may require the participation of the non-heme Fe_B, with the development of a catalytic current near its midpoint redox potential (−369 mV vs. NHE [37]). This is also supported by the extreme low redox potential value reported for a non-heme Fe nitrosyl model compound, which mimics the NOR non-heme Fe_B centre [50]. This evidence and the unchanged midpoint redox potential of the NOR catalytic heme b_3, under NO turnover, suggest the formation of a non-heme Fe nitrosyl (or dinitrosyl) species when NO is reduced [37]. On the other hand, O_2 reduction probably demands the formation of a heme b_3 Fe-O_2 complex, analogously to the terminal oxidases [36]. Therefore, the development of a catalytic current at the potential value close to the one reported for the heme b_3 midpoint redox potential (−162 mV vs. NHE [37]) is observed. The direct participation of heme b_3 on the NO reduction process will be discussed further. However, previous results have shown that the heme b_3 midpoint redox potential is not altered when the enzyme reduces NO, which implies that heme b_3 probably maintains its axial ligands during NO turnover [37]. The catalytic current shape and intensity are related to the turnover rate and number of electrons involved in the reduction process amongst other factors, such as the mass transport regime and the interfacial electron transfer. In the case of NO, since NOR presents higher turnover for NO reduction rather than for O_2 (Table 1), in the tested experimental conditions, namely the range of the electrode rotation speed values, it is not unexpected that the sigmoidal shape is less pronounced under NO turnover (Fig. 2 — panel C). Also, O_2 reduction not only has a smaller turnover but additionally has twice the electrons involved in the process, showing a different catalytic profile, with a more intense and better defined catalytic current than the NO reduction process (Fig. S.2).

3.4. NO reduction activity in solution and immobilised system

NO reduction activity was conducted with *Ps. nautica* NOR in solution, receiving electrons directly from its physiological electron donor (reduced cyt. c_{552}), monitoring the substrate consumption. Initial rates were determined for every assay. For all the deduced rate equations (see supporting information), steady-state and initial rate conditions were assumed. The experiments performed with the isolated NOR and

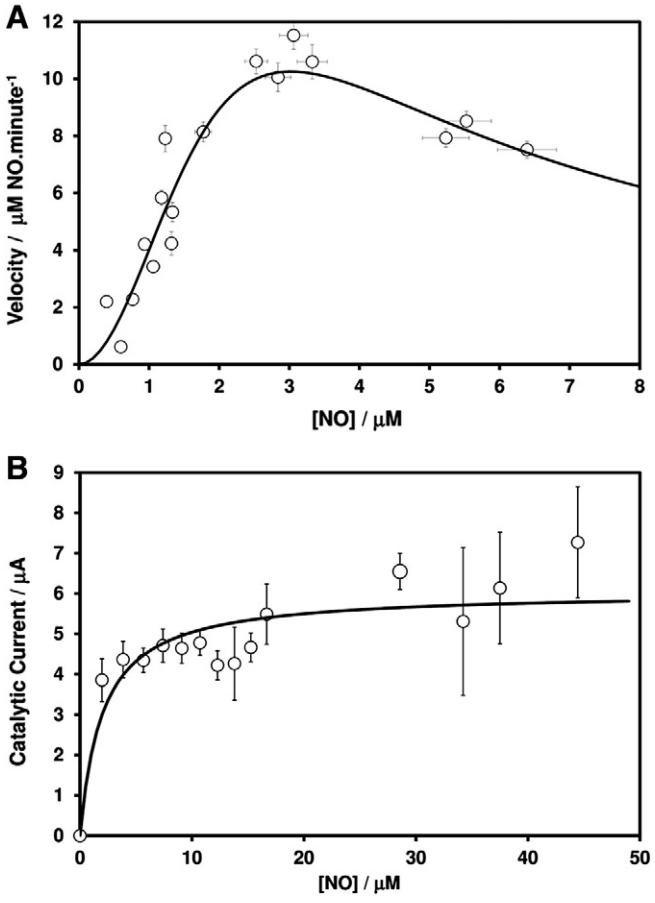

Fig. 3. Substrate dependence of NO reduction for the *Ps. nautica* NOR: A — NOR in solution using reduced cyt. c_{552} and B — immobilised NOR on a graphite RDE (experimental details described in the Materials and methods section).

the reduced cyt. c_{552} in the presence of NO revealed a substrate inhibition profile (Fig. 3A). The correspondent Hanes–Woolf and double reciprocal plots of the experimental data revealed the shape of a parabola and hyperbola, characteristic for a substrate inhibition profile [51] (see supplementary information — Fig. S.3).

In order to fit the experimental data shown in Fig. 3A, the following simplified kinetic model was assumed under NO turnover:

$$E_{red} + NO \overset{K_1}{\leftrightarrow} E(NO) + NO \overset{K_2}{\leftrightarrow} E(NO)_2 \overset{k_{cat}}{\rightarrow} E_{ox} + N_2O \quad (1)$$

$$E_{red} + NO \overset{Ki}{\leftrightarrow} E(NO)_i. \quad (2)$$

Eq. (1) describes the overall reaction catalysed by the enzyme in the presence of NO, with the consecutive binding of two substrate molecules to the enzyme active form, and consequent formation of N_2O [18]. In this work, E_{red} represents the enzyme fully reduced state (heme *c* Fe^{II}/heme *b* Fe^{II}/heme b_3 Fe^{II}/Fe^{II}_B), characterised as the enzyme active state [6]. The centre presents two possible substrate binding sites and the coordination of a NO molecule to the enzyme active form in an incorrect order which could lead to the formation of a non-reactive species (Eq. (2)). If this is the case, a high compulsory order on the substrate binding is required (see text below). The velocity equation for the proposed mechanism was deduced (Eq. (3)) and used to fit the experimental data, as shown in Fig. 3A. The best fit is presented in the same figure (Fig. 3A) with a solid line, and the correspondent kinetic parameters are listed in Table 1. The determined constants are in agreement with previous reports for the same [6] and other isolated bacterial NORs [11,15].

$$v = \frac{k_{cat}[E]_T}{\left(1 + \frac{K_2}{[NO]} + \frac{K_1K_2}{[NO]^2} + \frac{K_1K_2}{K_i[NO]}\right)}. \quad (3)$$

Steady-state kinetics under NO concentrations, with the immobilised *Ps. nautica* NOR and using the electrode as the electron donor, show a kinetic profile different from the previous presented when using the reduced cyt. c_{552} (Fig. 3B). The variations on the obtained catalytic currents were plotted as function of substrate concentration (Fig. 3B). Scan rate and electrode rotation dependence were performed in order to assure a convective flow to the electrode, eliminating substrate mass transfer limitations. The different kinetic profiles are detected in the lower NO concentrations (until 8 μM) or in the higher range (see supplementary information — Fig. S.4).

When using the electrode as the biochemical partner, the experimental data obtained under NO reduction (Fig. 3B) describes a hyperbolic behaviour tolerating higher substrate concentrations. On the other hand, since the enzyme presents a high turnover it becomes very difficult to achieve reproducible results on the lower substrate concentration level. The simplified kinetic model assumed was expressed previously in Eq. (1). A mathematical equation can be deduced (see supporting information) for the measured current intensity, which is proportional to the substrate reduction rate [49]. The deduced kinetic equation is presented below (Eq. (4)), and the best fit to the experimental data is presented in Fig. 3B (solid line), with the correspondent kinetic features indexed in Table 1.

$$I = \frac{I_{max}}{\left(1 + \frac{K_2}{[NO]} + \frac{K_1K_2}{[NO]^2}\right)}. \quad (4)$$

Since substrate concentration is higher than K_1 or K_2 ($S > K_1$ and $S > K_2$), the substrate saturation condition is ensured, so $I \cong I_{max} = nFAk_{cat}\Gamma$, where n is the number of electrons exchanged ($n = 2$), F the Faraday constant (96485C.mol.$^{-1}$), A the electrode area (geometric area 0.126 cm^2) and Γ the electrode coverage ($\Gamma = 2.16 \times 10^{-11}$ mol cm^{-2}). Therefore, the turnover rate constant k_{cat} can be estimated and compared with the previous determined with the enzyme in solution (see Table 1 and Results and discussion section, respectively). For both electron donor systems, the binding of the two substrate molecules to the enzyme catalytic centre is assumed to occur as a two consecutive steps, based on the knowledge of the NOR crystal structure, which presents a short Fe–Fe distance in its catalytic cavity (3.9 Å). Consequently, it is proposed that two NO molecules can be accommodated, but only after rearrangements on the catalytic centre [15]. The different dissociation constants for the substrate binding observed in the two electron donor systems (Table 1) and the different kinetic profiles can be related with the electron pathways for the catalytic site. When reduced cyt. c_{552} is used as electron donor, it is proposed that this protein docks with the NorC subunit, being the electrons transferred from there to the binuclear catalytic centre via the low-spin heme *b*. When the enzyme is immobilised on the electrode surface, electrons can flow directly from the electrode towards the catalytic di-iron site [37].

3.5. The NO inhibitory profile

NOR kinetic studies performed over time have shown an inhibitory profile on the lower substrate concentration range [11,38]. The model we propose describes a highly compulsory ordered mechanism, where the substrate binding order is relevant, because: 1) if the first substrate molecule is not bond to the correct iron site, an inhibited species can be formed, probably a heme b_3 Fe^{II}-NO complex, 2) in the enzyme active

form (fully reduced state) the catalytic heme b_3 is in a low-spin state with the permanence of the oxo-bridge [6], that breaks before or after substrate coordination and 3) the catalytic di-iron centre presents a short Fe–Fe distance making impossible to accommodate two NO molecules at the same time, without rearrangements upon the first NO molecule binding [15]. The transition of a substrate inhibition to a hyperbolic kinetic profile strongly suggests that this inhibition is due to an intramolecular ET rather than the formation of a heme b_3 Fe^{III}-NO complex, as previously proposed [11]. The disappearance of the inhibition profile when the enzyme is adsorbed to the electrode, can be explained by the quick/efficient electron transfer between the catalytic centre and the electrode (c.a. 73 s^{-1} [37]). Lachmann and co-workers [39] used spectroscopic methods to determined re-oxidation rate constants of the NOR metal co-factors under NO turnover, however, the determined values present substrate concentration dependence and are lower (c.a. 12 s^{-1} [39]) than the ones determined for the direct ET between the enzyme and the graphite electrode [37].

3.6. Oxygen reduction activity in solution and immobilised system

Oxidoreductase activity was also studied with the *Ps. nautica* NOR, using the same approaches as described for its natural substrate. The data were obtained with the previous mentioned electron donors (reduced cyt. c_{552} in solution and immobilised NOR on a graphite RDE) and the result treatment was done as stated for NO reduction.

Data obtained in the presence of O_2 equally describe a substrate inhibition (Fig. 4A and B), independently from the redox partner used.

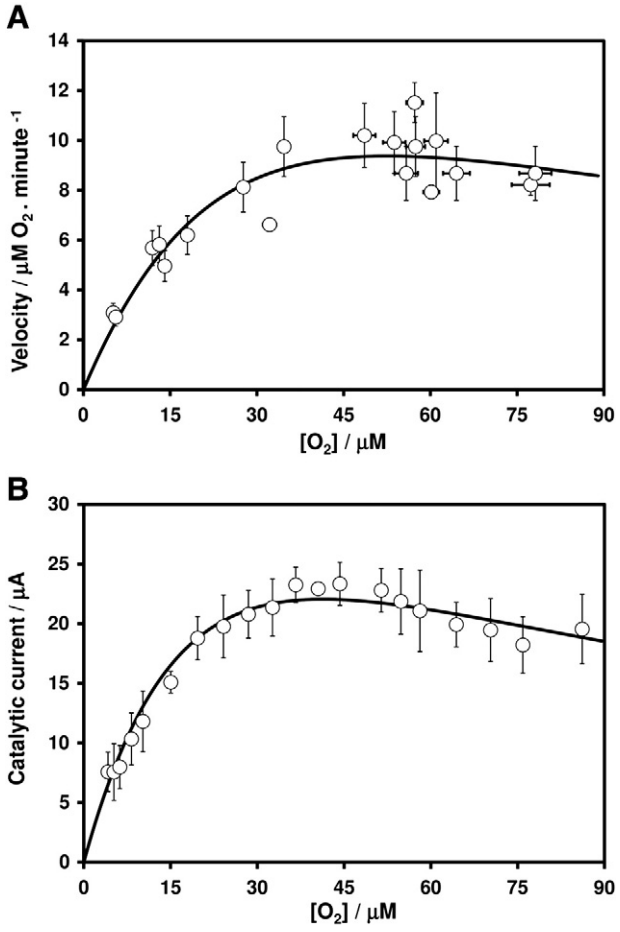

Fig. 4. Substrate dependence of O_2 reduction for the *Ps. nautica* NOR: A — NOR in solution using reduced cyt. c_{552} and B — immobilised NOR on a graphite RDE (experimental details described in the Materials and methods section).

Due to the substrate stoichiometry, an appropriate kinetic model was considered and explained by Eqs. (4) and (5):

$$E_{red} + O_2 \overset{K_1}{\leftrightarrow} EO_2 \overset{k_{cat}}{\rightarrow} E_{ox} + H_2O \quad (5)$$

$$EO_2 + O_2 \overset{Ki}{\leftrightarrow} E(O_2)_2. \quad (6)$$

The model shows a simplified representation for O_2 reduction. Eq. (5) describes the binding of one substrate molecule to the enzyme active form and consequent water formation. We propose the binding of a second substrate molecule to the enzyme active centre with the consequent development of a substrate inhibition scenario with the formation of a non-reactive species (Eq. (6)), decreasing the substrate reduction rate, as observed experimentally, see Fig. 4A and B. In the presence of the reduced cyt. c_{552} in solution, the simplest velocity equation based on the proposed mechanism is translated by Eq. (7) [51] and the best fit to the experimental data is shown in Fig. 4A, with the kinetic parameters summarised in Table 1 and compared further.

$$v = \frac{k_{cat}[E]_t[O_2]}{\left(K_1 + [O_2] + \frac{[O_2]^2}{K_i}\right)}. \quad (7)$$

Steady-state kinetic studies in the presence of O_2 have been reported using chemical electron donors [18,21], or applying flow-flash technique, in single turnover experiments [19], but this is the first report showing steady-state oxidoreductase activity of an isolated bacterial NOR with its physiological electron donor.

With the NOR immobilised on a graphite RDE, in the presence of O_2 as the substrate (Fig. 4B), the data show an identical inhibitory profile, as previously described for the assay with the cyt. c_{552} (Fig. 4A). The same kinetic model was used (Eqs. (4) and (5)), with the correspondent deduced equation expressed in terms of catalytic current and used to fit the experimental data (Eq. (8)).

$$I = \frac{I_{max}[O_2]}{\left(K_1 + [O_2] + \frac{[O_2]^2}{K_i}\right)}. \quad (8)$$

In this specific case, k_{cat} is unable to be estimated correctly, since the total enzyme adsorbed to the electrode is much lower than the amount used in the experiments conducted in solution, and required for a linear catalytic response (0.5 μM). According to Table 1, the determined kinetic parameters under O_2 reduction are similar to the previous determined ones, which can point to the same inhibition process for the O_2 reduction mechanism. This shows that the intramolecular electron transfer rate is not limiting the O_2 reduction process, as proposed for NO reduction. The mechanism for O_2 reduction by this class of enzymes has not been elucidated yet, but it is proposed to be analogous to the HCuO mechanism, involving the O_2 binding to the catalytic heme b_3. Since a non-allosteric site was reported for NOR, the inhibited species can be due to the binding of an O_2 molecule to the catalytic site, namely the non-heme Fe_B, resulting in a modified conformation of the catalytic site, enabling the catalysis, or the presence of a substrate molecule near the catalytic heme b_3. A detailed characterisation on the O_2 reduction in the NOR di-iron site demands more experiments to confirm these assumptions.

3.7. pH dependence experiments

The kinetic experiments using the immobilised RDE *Ps. nautica* NOR, in the presence of NO, under pH dependence exhibited a typical bell shape curve (Fig. 5), usually seen in pH dependence experiment [51]. For the first time, the pH scale was enlarged to more acidic pH values. Previous reports were only focused on the neutral and basic part of the pH scale, from pH 5 to 9 [19,21].

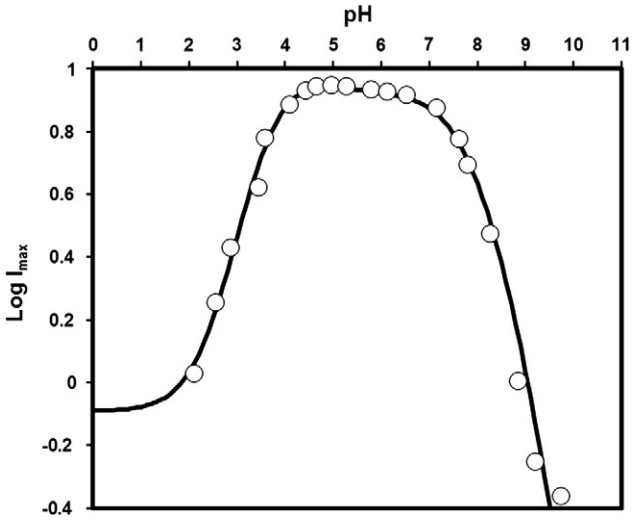

Fig. 5. pH dependence of *Ps. nautica* NOR under NO turnover, preformed with the enzyme immobilised on a graphite RDE.

At every pH value, NOR kinetic profile was evaluated and a theoretical line was fitted, using the model described by Eq. (1) (with the correspondent rate equation — Eq. (7)). Different kinetic models with only three or four protonable residues were assessed (supporting information — Fig. S.5A and S.5B), but the best residual plot was achieved employing five ionisable residues (Fig. S.6) as presented in Scheme 1. Our own previous electrochemical studies on *Ps. nautica* NOR performed in non-turnover conditions, revealed the presence of five protonable groups on the catalytic binuclear centre vicinity [37]. These residues can be responsible for modulating the chemical environment of the catalytic irons and therefore influence the catalytic response. With this, a kinetic mechanism considering five protonated forms, beginning from the model described in Eq. (1) was assumed and it is described in Scheme 1.

As previously, in the kinetic mechanism the enzyme active form was assumed to be the reduced catalytic di-iron site (E_{red}). The protein global charge was assumed neutral in one of the protonated forms (as a formalism), with variation on the global charge due to the protonation/deprotonation. The dissociation constant designations are presented as the Michaelis–Menten formalism (pK_{an}). The three proton enzyme form (H_3-E_{red}, in Scheme 1) considered to be more active, therefore, the turnover rates of the other enzymatic forms with ability to catalyse the substrate are affected by an adjustment parameter (β), commonly introduced in kinetic systems to improve the fitting to the proposed model.

A simplification of this model (Scheme 1) can be assumed, since K_1 and K_2 are much lower than the substrate concentration (K_1 and $K_2 \ll$ [NO]), leading to two assumptions: 1) the equilibrium presented in Eq. (1) is right shifted, with the total amount of enzyme approximately equal to the enzyme form bound to the substrate (with two substrate molecules) and 2) for NO concentration higher than K_1 and K_2, the rate for NO reduction is approximately equal to I'_{max}. Therefore, the kinetic model can be resumed to Scheme 1-grey box and the kinetic expression

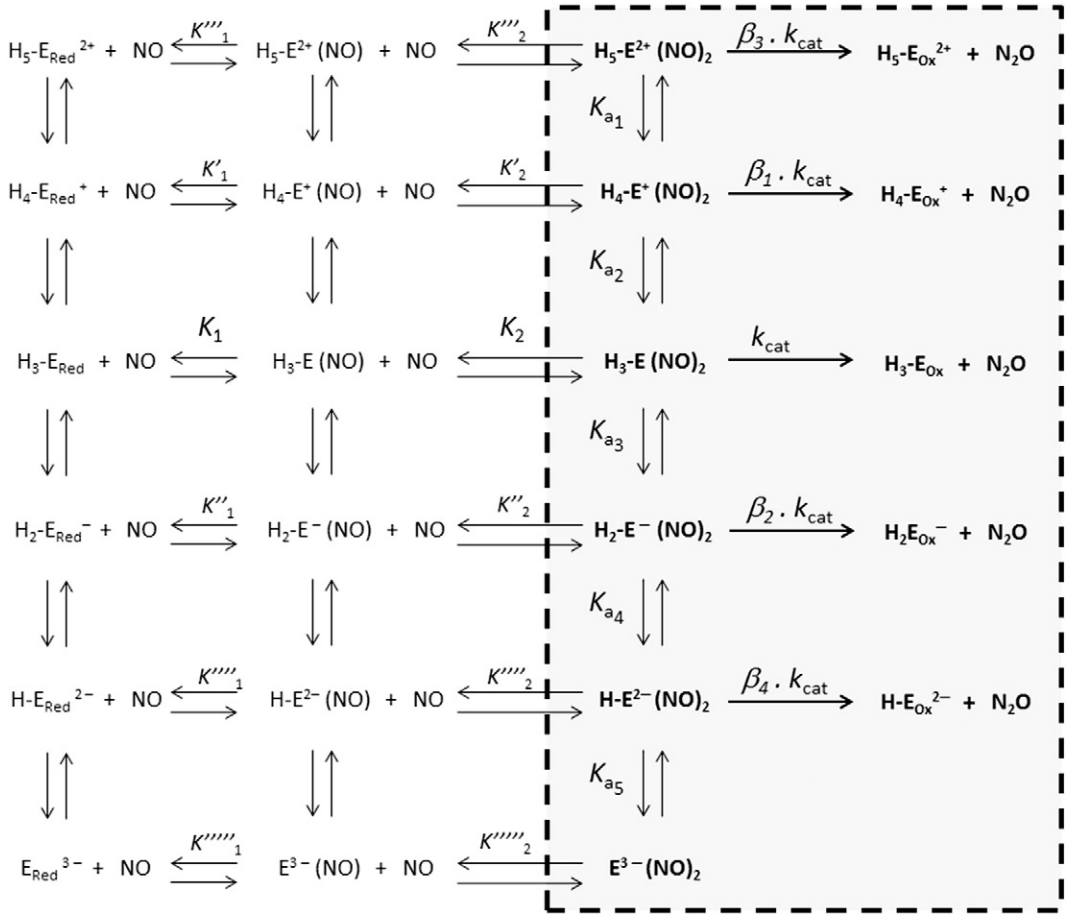

Scheme 1. Kinetic model for the *Ps. nautica* NOR with five dissociable groups. Only the non-protonated form is catalytic inactive. The three protonated forms show the higher catalytic turnover, and the remaining protonated forms show their k_{cat} affected by different adjustment parameters — β_1 to β_4.

for the catalytic response in terms of pH dependence is given by Eq. (9), which is totally independent of the dissociation constants for substrate binding.

$$I = \frac{\left(1 + \beta_1 \frac{[H^+]}{K_{a_2}} + \beta_2 \frac{K_{a_3}}{[H^+]} + \beta_3 \frac{[H^+]^2}{K_{a_1} K_{a_2}} + \beta_4 \frac{K_{a_3} K_{a_4}}{[H^+]^2}\right) I'_{max}}{\left(1 + \frac{[H^+]^2}{K_{a_1} K_{a_2}} + \frac{[H^+]}{K_{a_2}} + \frac{K_{a_3}}{[H^+]} + \frac{K_{a_3} K_{a_4}}{[H^+]^2} + \frac{K_{a_3} K_{a_4} K_{a_5}}{[H^+]^3}\right)}. \quad (9)$$

The best fit to the data is exhibited in Fig. 5 (solid line), with the following parameters: $pK_{a1} = 3.47 \pm 0.35$, $pK_{a2} = 4.50, \pm 0.59$, $pK_{a3} = 5.27 \pm 0.61$, $pK_{a4} = 7.70 \pm 0.79$, $pK_{a5} = 8.64 \pm 0.81$, $\beta_1 = 0.99 \pm 0.10$, $\beta_2 = 0.93 \pm 0.09$, $\beta_3 = 0.09 \pm 0.05$ and $\beta_4 = 0.36 \pm 0.04$. This is in agreement with the kinetic profile previously published by other authors [21], at least at higher pH values.

The pK_a values achieved are in agreement with the values determined in non-turnover conditions [37], while the adjustment parameters (β_1 and β_2) show that there is no considerable difference in the catalytic activity between the two, three and four protonated forms. Therefore, we do believe that residues containing dissociable groups near the di-iron catalytic centre vicinity are responsible for modulating the binuclear iron centre potential as well as the chemical environment. Some residues can be crucial, not only for substrate binding, reduction and diffusion towards the catalytic site, but also essential for electron transfer from the heme ET centres (hemes *b* and *c*) and proton transfer from the periplasmic side of the membrane, through the transmembrane polypeptide chain, until it reaches the catalytic centre.

3.8. New insights on the catalytic mechanism of NO reduction

There is an intense discussion concerning the mechanism of enzymatic reduction of NO by NORs. Different hypothetical mechanisms are still in debate and until now there is no unequivocal proof that elects or disclaims one of proposed models. Based on the presented results, we revised the mechanism proposing, for NO reduction, the consecutive binding of two substrate molecules to the di-iron site (Scheme 2). The lack of the characterisation of relevant catalytic intermediates for NO reduction leads us to consider both *cis* and *trans*-mechanisms. The enzyme active form is proposed to be the fully reduced state (Scheme 2-a), with both catalytic iron sites in the ferrous state [6]. The binding of NO to the non-heme Fe_B could force the opening of the oxo/hydroxo bridge, leaving this group bound to the Fe^{II}-heme b_3 (Scheme 2-b). The formation of this first catalytic intermediate is favourable since high-spin non-heme $[FeNO]^7$ compounds show a strong and stable Fe – NO bond, corresponding almost to a covalent interaction [25], while the ferrous-heme nitrosyl complexes are also stable but quite unreactive [52]. The existence of the hydroxyl group on the catalytic heme b_3

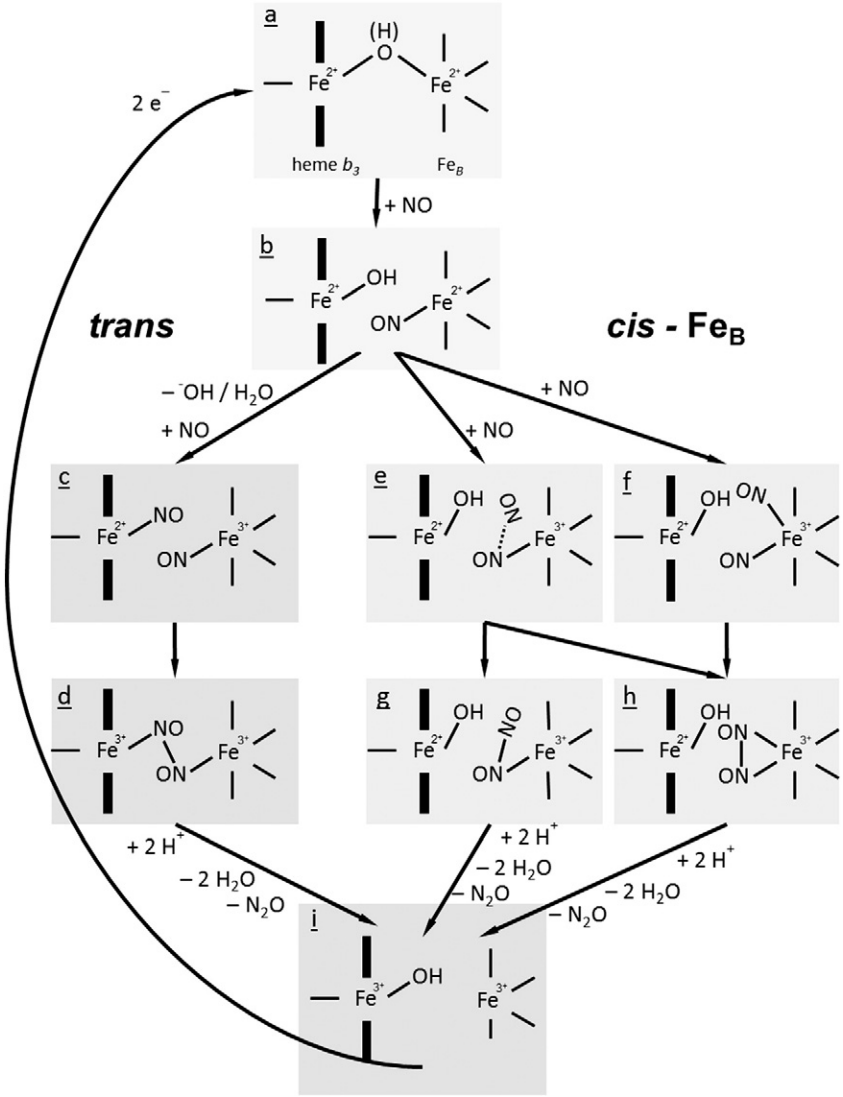

Scheme 2. NO reduction mechanism with the *trans* and *cis*-Fe_B models. The *cis*-Fe_B mechanism is presented with the possibility of one or both NO molecules binding to the non-heme iron.

axial position would protect this iron site reactivity towards NO, as it could be used to orientate the entrance of a second NO molecule, or to stabilise a Fe_B-hyponitrite formation (see text below). This is also supported by the electrochemical studies developed in our research group, which show an unchanged heme b_3 midpoint redox potential during NO turnover [37].

From this first intermediate species, the Fe^{II}_B-mononitrosyl (Scheme 2-b), we can envisage the two assumed mechanisms. Assuming a *trans*-mechanism, the protonation or removal of the hydroxyl group on the heme b_3 site would produce the water formation, leaving the ferrous heme b_3 site free to coordinate the second NO molecule (Scheme 2-c), which can go further into the NO reduction, with the hyponitrite formation between the two Fe sites (Scheme 2-d), and after a double protonation this intermediate could release a water molecule and N_2O, the reaction product. The di-iron centre, after suffering rearrangements can restore the catalytic centre initial form, now on a ferric form (Scheme 2-i), ready for the next turnover. Kumita et al. published an EPR characterisation of freeze-quenching samples and found transition reaction intermediates prior to N_2O formation, supporting the supposed *trans*-mechanism [5]. However, the replacement of the hydroxyl group for a substrate molecule should produce a shift on the catalytic heme midpoint redox potential (as discussed earlier in the text), which has not been detected yet, and so, this is contrary to the postulated on the *trans*-mechanism [37].

The same first intermediate (Fe^{II}_B-NO — Scheme 2-b) can react with the second NO molecule, without displacement of the OH group coordinated to the catalytic heme Fe site. So in a *cis*-Fe_B mechanism, the second substrate molecule can coordinate to the Fe_B site or only approach the catalytic cavity enough to react and form a Fe_B-dinitrosyl/Fe_B-hyponitrite complex, respectively (see Scheme 2-e and f). The remaining hydroxyl group, beyond protecting the heme Fe site against NO and orientating the second NO molecule (Scheme 2-g and h), can be essential for: 1) stabilising the Fe_B-dinitrosyl/Fe_B-hyponitrite species formed and 2) transferring the reducing equivalents from the heme b_3 Fe site, with the consequent oxygen atom abstraction, enhancing the N – N bond formation.

Dinitrosylated iron complexes have been intensively studied, since they are relevant in biological systems, and often common in Fe-Sulfur clusters [53,54]. In general, Fe-nitrosylated species are more frequent in five or six-coordinating systems while dinitrosylated forms seem to be more common in lower coordination environments, with four or five coordination ligands [55,56]. Making a closer observation of the cNOR non-heme Fe_B site, which presents a three histidine and a glutamate coordination, it does not seem probable the formation of a Fe_B-dinitrosyl complex, due to the high number of coordinating ligands. Also, studies on the modified sperm whale myoglobin indicated that only two histidines and a glutamate residue are essential for the non-heme Fe_B coordination and consequent NO reduction [57].

It is our conviction that a *cis*-Fe_B mechanism is more favourable, since the remaining hydroxyl group coordinated to the heme b_3 can be seen as a major key step on the NO reduction mechanism, being responsible for hyponitrite formation and/or stabilisation, as well as assisting on the H_2O molecule abstraction, triggering the N_2O release from the catalytic centre.

The mechanism indicated in Scheme 2, proposes a few hypothetical catalytic intermediates that have not been identified yet, and further studies focusing on the reaction intermediates detection should be attained in the future.

4. Concluding remarks

In this work it is presented, for the first time, a complete steady-state kinetic study on NOR in the presence of both substrates NO and O_2, in which the correspondent kinetic parameters were determined. The assays were done in the presence of the natural electron donor, the cyt. c_{552} (in close physiological conditions), or using an alternative electron donor system, a graphite rotating electrode mimicking the enzyme redox partner. The enzyme affinity for both substrates was evaluated, as well as the turnover, confirming a higher value for NO reduction and the residual activity of NOR for O_2. The observed kinetic behaviour under high NO concentrations, in conditions where the enzyme is immobilised, shows that NOR can perform NO reduction with a similar turnover, without an inhibitory effect, observed in the solution assays using cyt. c_{552} as redox partner. The inhibition at lower substrate concentrations was attributed to the enzyme intramolecular electron transfer rate limitations. Investigation of the NOR activity under pH dependence was obtained for the first time on lower pH values, showing the relevance of the ionisable residues/groups surrounding the binuclear catalytic centre which can modulate the di-iron catalytic centre redox potential and reactivity.

The kinetic and electrochemical studies conducted allow new insights into the O_2 and NO reduction mechanism, with the possibility of revising the latter one. From the results, it seems presumable that the mechanism for NO reduction requires the binding of the two substrate molecules in two consecutive steps. Therefore we propose the formation of a Fe_B-mononitrosyl, as the first catalytic intermediate, which can evolve to a Fe_B-dinitrosyl/Fe_B-hyponitrite, in a *cis*-Fe_B catalytic mechanism or to a $[FeNO]^7{}_2$ species, supporting a trans-mechanism. Further studies are necessary to detect the possible catalytic intermediates.

Acknowledgements

We would like to thank Fundação para a Ciência e Tecnologia for the financial support through grants SFRH/BD/39009/2007 (AGD), PDTC/QUI/64638/2006 (IM) and PDCT/QUI-BIOQ/1/6481/2010 (IM). REQUIMTE is funded by grant PEst-C/EQB/LA0006/2013 from FCT/MEC.

Appendix A. Supplementary data

Supplementary data to this article can be found online at http://dx.doi.org/10.1016/j.bbabio.2014.01.001.

References

[1] J. Hoglen, T.C. Hollocher, Purification and some characteristics of nitric oxide reductase-containing vesicles from Paracoccus denitrificans, J. Biol. Chem. 264 (1989) 7556–7563.
[2] G.J. Carr, S.J. Ferguson, The nitric oxide reductase of Paracoccus denitrificans, Biochem. J. 269 (1990) 423–429.
[3] B. Heiss, K. Frunzke, W.G. Zumft, Formation of the N – N bond from nitric oxide by a membrane-bound cytochrome bc complex of nitrate-respiring (denitrifying) Pseudomonas stutzeri, J. Bacteriol. 171 (1989) 3288–3297.
[4] D.H. Kastrau, B. Heiss, P.M. Kroneck, W.G. Zumft, Nitric oxide reductase from Pseudomonas stutzeri, a novel cytochrome bc complex. Phospholipid requirement, electron paramagnetic resonance and redox properties, Eur. J. Biochem. 222 (1994) 293–303.
[5] H. Kumita, K. Matsuura, T. Hino, S. Takahashi, H. Hori, Y. Fukumori, I. Morishima, Y. Shiro, NO reduction by nitric-oxide reductase from denitrifying bacterium Pseudomonas aeruginosa: characterization of reaction intermediates that appear in the single turnover cycle, J. Biol. Chem. 279 (2004) 55247–55254.
[6] C.G. Timoteo, A.S. Pereira, C.E. Martins, S.G. Naik, A.G. Duarte, J.J. Moura, P. Tavares, B.H. Huynh, I. Moura, Low-spin heme b3 in the catalytic center of nitric oxide reductase from Pseudomonas nautica, Biochemistry 50 (2011) 4251–4262.
[7] M.C. Marquez, A. Ventosa, Marinobacter hydrocarbonoclasticus Gauthier, et al. 1992 and Marinobacter aquaeolei Nguyen et al. 1999 are heterotypic synonyms, Int. J. Syst. Evol. Microbiol. 55 (2005) (1992) 1349–1351.
[8] W.G. Zumft, Nitric oxide reductases of prokaryotes with emphasis on the respiratory, heme-copper oxidase type, J. Inorg. Biochem. 99 (2005) 194–215.
[9] P. Tavares, A.S. Pereira, J.J. Moura, I. Moura, Metalloenzymes of the denitrification pathway, J. Inorg. Biochem. 100 (2006) 2087–2100.
[10] N.J. Watmough, S.J. Field, R.J. Hughes, D.J. Richardson, The bacterial respiratory nitric oxide reductase, Biochem. Soc. Trans. 37 (2009) 392–399.
[11] P. Girsch, S. de Vries, Purification and initial kinetic and spectroscopic characterization of NO reductase from Paracoccus denitrificans, Biochim. Biophys. Acta 1318 (1997) 202–216.
[12] J. Hendriks, A. Warne, U. Gohlke, T. Haltia, C. Ludovici, M. Lubben, M. Saraste, The active site of the bacterial nitric oxide reductase is a dinuclear iron center, Biochemistry 37 (1998) 13102–13109.

[13] M.R. Cheesman, W.G. Zumft, A.J. Thomson, The MCD and EPR of the heme centers of nitric oxide reductase from Pseudomonas stutzeri: evidence that the enzyme is structurally related to the heme-copper oxidases, Biochemistry 37 (1998) 3994–4000.
[14] P. Moënne-Loccoz, O.M.H. Richter, H.W. Huang, I.M. Wasser, R.A. Ghiladi, K.D. Karlin, S. Vries, Nitric oxide reductase from Paracoccus denitrificans contains an oxo-bridged heme/non-heme diiron center, J. Am. Chem. Soc. 122 (2000) 9344.
[15] T. Hino, Y. Matsumoto, S. Nagano, H. Sugimoto, Y. Fukumori, T. Murata, S. Iwata, Y. Shiro, Structural basis of biological N2O generation by bacterial nitric oxide reductase, Science 330 (2010) 1666–1670(New York, N.Y.).
[16] C. Butler, E. Forte, F. Maria Scandurra, M. Arese, A. Giuffre, C. Greenwood, P. Sarti, Cytochrome bo(3) from Escherichia coli: the binding and turnover of nitric oxide, Biochem. Biophys. Res. Commun. 296 (2002) 1272–1278.
[17] T. Fujiwara, Y. Fukumori, Cytochrome cb-type nitric oxide reductase with cytochrome c oxidase activity from Paracoccus denitrificans ATCC 35512, J. Bacteriol. 178 (1996) 1866–1871.
[18] N. Sakurai, T. Sakurai, Isolation and characterization of nitric oxide reductase from Paracoccus halodenitrificans, Biochemistry 36 (1997) 13809–13815.
[19] U. Flock, N.J. Watmough, P. Adelroth, Electron/proton coupling in bacterial nitric oxide reductase during reduction of oxygen, Biochemistry 44 (2005) 10711–10719.
[20] C.M. Cordas, A.S. Pereira, C.E. Martins, C.G. Timoteo, I. Moura, J.J. Moura, P. Tavares, Nitric oxide reductase: direct electrochemistry and electrocatalytic activity, Chembiochem 7 (2006) 1878–1881.
[21] U. Flock, P. Lachmann, J. Reimann, N.J. Watmough, P. Adelroth, Exploring the terminal region of the proton pathway in the bacterial nitric oxide reductase, J. Inorg. Biochem. 103 (2009) 845–850.
[22] J. Reimann, U. Flock, H. Lepp, A. Honigmann, P. Adelroth, A pathway for protons in nitric oxide reductase from Paracoccus denitrificans, Biochim. Biophys. Acta 1767 (2007) 362–373.
[23] P. Moenne-Loccoz, Spectroscopic characterization of heme iron-nitrosyl species and their role in NO reductase mechanisms in diiron proteins, Nat. Prod. Rep. 24 (2007) 610–620.
[24] S.J. Field, F.H. Thorndycroft, A.D. Matorin, D.J. Richardson, N.J. Watmough, The respiratory nitric oxide reductase (NorBC) from Paracoccus denitrificans, Methods Enzymol. 437 (2008) 79–101.
[25] T. Berto, A.L. Speelman, S. Zheng, N. Lehnert, Mono- and dinuclear non-heme iron-nitrosyl complexes: models for key intermediates in bacterial nitric oxide reductases, Coord. Chem. Rev. 257 (2012) 255–259.
[26] S. Zheng, T.C. Berto, E.W. Dahl, M.B. Hoffman, A.L. Speelman, N. Lehnert, The functional model complex [Fe(BPMP)(OPr)(NO)](BPh) provides insight into the mechanism of flavodiiron NO reductases, J. Am. Chem. Soc. 135 (2013) 4902–4905.
[27] K.L. Gronberg, M.D. Roldan, L. Prior, G. Butland, M.R. Cheesman, D.J. Richardson, S. Spiro, A.J. Thomson, N.J. Watmough, A low-redox potential heme in the dinuclear center of bacterial nitric oxide reductase: implications for the evolution of energy-conserving heme-copper oxidases, Biochemistry 38 (1999) 13780–13786.
[28] M.R. Blomberg, P.E. Siegbahn, Mechanism for N(2)O generation in bacterial nitric oxide reductase: a quantum chemical study, Biochemistry 51 (2012) 5173–5186.
[29] P. Moenne-Loccoz, S. de Vries, Structural characterization of the catalytic high-spin heme b of nitric oxide reductase: a resonance Raman study, J. Am. Chem. Soc. 120 (1998) 5147–5152.
[30] J.H. Hendriks, A. Jasaitis, M. Saraste, M.I. Verkhovsky, Proton and electron pathways in the bacterial nitric oxide reductase, Biochemistry 41 (2002) 2331–2340.
[31] T. Hino, S. Nagano, H. Sugimoto, T. Tosha, Y. Shiro, Molecular structure and function of bacterial nitric oxide reductase, Biochim. Biophys. Acta 1817 (2011) 680–687.
[32] J.P. Collman, A. Dey, Y. Yang, R.A. Decreau, T. Ohta, E.I. Solomon, Intermediates involved in the two electron reduction of NO to N2O by a functional synthetic model of heme containing bacterial NO reductase, J. Am. Chem. Soc. 130 (2008) 16498–16499.
[33] N. Yeung, Y.W. Lin, Y.G. Gao, X. Zhao, B.S. Russell, L. Lei, K.D. Miner, H. Robinson, Y. Lu, Rational design of a structural and functional nitric oxide reductase, Nature 462 (2009) 1079–1082.
[34] Y.W. Lin, N. Yeung, Y.G. Gao, K.D. Miner, S. Tian, H. Robinson, Y. Lu, Roles of glutamates and metal ions in a rationally designed nitric oxide reductase based on myoglobin, Proc. Natl. Acad. Sci. U. S. A. 107 (2010) 8581–8586.
[35] T. Hayashi, K.D. Miner, N. Yeung, Y.W. Lin, Y. Lu, P. Moenne-Loccoz, Spectroscopic characterization of mononitrosyl complexes in heme–nonheme diiron centers within the myoglobin scaffold (Fe(B)Mbs): relevance to denitrifying NO reductase, Biochemistry 50 (2011) 5939–5947.
[36] S. Yoshikawa, K. Muramoto, K. Shinzawa-Itoh, M. Mochizuki, Structural studies on bovine heart cytochrome c oxidase, Biochim. Biophys. Acta 1817 (2012) 579–589.
[37] C.M. Cordas, A.G. Duarte, J.J. Moura, I. Moura, Electrochemical behaviour of bacterial nitric oxide reductase-evidence of low redox potential non-heme Fe(B) gives new perspectives on the catalytic mechanism, Biochim. Biophys. Acta 1827 (2013) 233–238.
[38] M. Koutny, I. Kucera, Kinetic analysis of substrate inhibition in nitric oxide reductase of Paracoccus denitrificans, Biochem. Biophys. Res. Commun. 262 (1999) 562–564.
[39] P. Lachmann, Y. Huang, J. Reimann, U. Flock, P. Adelroth, Substrate control of internal electron transfer in bacterial nitric-oxide reductase, J. Biol. Chem. 285 (2010) 25531–25537.
[40] M. Prudencio, A.S. Pereira, P. Tavares, S. Besson, I. Cabrito, K. Brown, B. Samyn, B. Devreese, J. Van Beeumen, F. Rusnak, G. Fauque, J.J. Moura, M. Tegoni, C. Cambillau, I. Moura, Purification, characterization, and preliminary crystallographic study of copper-containing nitrous oxide reductase from Pseudomonas nautica 617, Biochemistry 39 (2000) 3899–3907.
[41] G. Fauque, J.J.G.S. Besson, L. Saraiva, I. Moura, Caractérisation préliminaire de système cytochromique de la bactérie marine dénitrifiante Pseudomonas nautica 617, Oceans 18 (1992) 211–216.
[42] R. Gilmour, C.F. Goodhew, G.W. Pettigrew, Cytochrome c' of Paracoccus denitrificans, Biochim. Biophys. Acta 1059 (1991) 233–238.
[43] M.T. Giudici-Orticoni, G. Leroy, W. Nitschke, M. Bruschi, Characterization of a new dihemic c(4)-type cytochrome isolated from Thiobacillus ferrooxidans, Biochemistry 39 (2000) 7205–7211.
[44] L.M. Saraiva, S. Besson, G. Fauque, I. Moura, Characterization of the dihemic cytochrome c549 from the marine denitrifying bacterium Pseudomonas nautica 617, Biochem. Biophys. Res. Commun. 199 (1994) 1289–1296.
[45] L.M. Saraiva, S. Besson, I. Moura, G. Fauque, Purification and preliminary characterization of three c-type cytochromes from Pseudomonas nautica strain 617, Biochem. Biophys. Res. Commun. 212 (1995) 1088–1097.
[46] L.M. Saraiva, G. Fauque, S. Besson, I. Moura, Physico-chemical and spectroscopic properties of the monohemic cytochrome C552 from Pseudomonas nautica 617, Eur. J. Biochem. 224 (1994) 1011–1017.
[47] D.R. Lide, CRC Handbook of Chemistry and Physics A Ready Reference Book of Chemical and Physical Data, 88th ed. CRC press, Taylor & Francis group, London, New York, 2007–2008.
[48] K. Conrath, A.S. Pereira, C.E. Martins, C.G. Timoteo, P. Tavares, S. Spinelli, J. Kinne, C. Flaudrops, C. Cambillau, S. Muyldermans, I. Moura, J.J. Moura, M. Tegoni, A. Desmyter, Camelid nanobodies raised against an integral membrane enzyme, nitric oxide reductase, Protein Sci. 18 (2009) 619–628.
[49] C. Leger, P. Bertrand, Direct electrochemistry of redox enzymes as a tool for mechanistic studies, Chem. Rev. 108 (2008) 2379–2438.
[50] T.C. Berto, M.B. Hoffman, Y. Murata, K.B. Landenberger, E.E. Alp, J. Zhao, N. Lehnert, Structural and electronic characterization of non-heme Fe(II)-nitrosyls as biomimetic models of the FeB Center of Bacterial Nitric Oxide Reductase (NorBC), J. Am. Chem. Soc. 133 (2011) 16714–16717.
[51] A. Cornish-Bowden, Fundamentals of Enzyme Kinetics, 3rd ed. Portland Press, London, 2004.
[52] L.E. Goodrich, F. Paulat, V.K. Praneeth, N. Lehnert, Electronic structure of heme-nitrosyls and its significance for nitric oxide reactivity, sensing, transport, and toxicity in biological systems, Inorg. Chem. 49 (2010) 6293–6316.
[53] F.T. Tsai, T.S. Kuo, W.F. Liaw, Dinitrosyl iron complexes (DNICs) bearing O-bound nitrito ligand: reversible transformation between the six-coordinate {Fe(NO)2}9 [(1-MeIm)2(eta(2)-ONO)Fe(NO)2] (g = 2.013) and four-coordinate {Fe(NO)2}9 [(1-MeIm)(ONO)Fe(NO)2] (g = 2.03), J. Am. Chem. Soc. 131 (2009) 3426–3427.
[54] C.C. Tsou, T.T. Lu, W.F. Liaw, EPR, UV–vis, IR, and X-ray demonstration of the anionic dimeric dinitrosyl iron complex [(NO)(2)Fe(micro-S(t)Bu)(2)Fe(NO)(2)](−): relevance to the products of nitrosylation of cytosolic and mitochondrial aconitases, and high-potential iron proteins, J. Am. Chem. Soc. 129 (2007) 12626–12627.
[55] J.D.M. Kurtz, Flavo-diiron enzymes: nitric oxide or dioxygen reductases? Dalton Trans. (2007) 4115–4121.
[56] B. D'Autreaux, O. Horner, J.L. Oddou, C. Jeandey, S. Gambarelli, C. Berthomieu, J.M. Latour, I. Michaud-Soret, Spectroscopic description of the two nitrosyl-iron complexes responsible for fur inhibition by nitric oxide, J. Am. Chem. Soc. 126 (2004) 6005–6016.
[57] Y.W. Lin, N. Yeung, Y.G. Gao, K.D. Miner, L. Lei, H. Robinson, Y. Lu, Introducing a 2-His-1-Glu nonheme iron center into myoglobin confers nitric oxide reductase activity, J. Am. Chem. Soc. 132 (2010) 9970–9972.